Journal of Molecular Structure 1288 (2023) 135754

Contents lists available at ScienceDirect

Journal of Molecular Structure

journal homepage: www.elsevier.com/locate/molstr

Synthesis, docking and evaluation of novel fused pyrimidine compounds as possible lead compounds with antibacterial and antitumor activities.

Rami Y. Morjan [a,1], Amany F. El-Hallaq [b], Jannat N. Azarah [a], Ihab M. Almasri [c,1], Mazen M. Alzaharna [d], Mariam R. Al-Reefi [e], Ian Beadham [f], Omar S. Abu-Teim [b], Abdelraouf A. Elmanama [d], Adel M. Awadallah [a], James Raftery [e], John M. Gardiner [g,*]

[a] Department of Chemistry, Islamic University of Gaza, P.O. Box108, Palestine
[b] Department of Chemistry, Al-Azhar University of Gaza, P.O. Box 1277, Palestine
[c] Faculty of Pharmacy, Department of Pharmaceutical Chemistry, Al-Azhar University of Gaza, P.O. Box 1277, Palestine
[d] Medical Laboratory Sciences Department, Faculty of Health Sciences, Islamic University of Gaza, P.O. Box108, Palestine
[e] Medical Laboratory Sciences Department, Faculty of Health Sciences, Israa University of Gaza, Gaza Strip, Palestine
[f] School of Life Sciences, Pharmacy and Chemistry, Kingston University London, Kingston upon Thames, London, UK
[g] Department of Chemistry, School of Natural Sciences, Faculty of Science and Engineering, The University of Manchester, Manchester M13 9PL, UK

A B S T R A C T

Reaction of a series of hydrazonoyl chlorides with substituted aminopyrimidines afforded good selectivity in most cases leading either to formation of new imidazo [1,2-a]pyrimidine derivatives, or regioisomeric hydrazonamide adducts. The compounds were evaluated for antibacterial and anticancer activities. Screening against *E. Coli, P. aeruginosa, S. aureus, S. epidermidis, B. subtilis* and *K. rhizophila* did identify several different compound types with MIC of 0.1-0.4 mg/mL. Anticancer evaluation against a HeLa cell line identified one imidazo[1,2-a]pyrimidine lead. An *in silico* target fishing analysis suggest three possible high value protein targets, Tankyrase-2 (Tank-2), Cyclin-dependent kinase (CDK2) and Epidermal growth factor tyrosine kinase receptor (EGFR), with modelling fit against co-crystallized known ligands. This provides a new structural family lead for further investigation of molecular targets and potential SAR activity development.

1. Introduction

The search continues unabated to identify new antimicrobial agents to meet the clinical need for new drugs which can clear infections from multi-drug resistant (MDR) pathogens. These pathogens have become increasingly difficult to treat with existing antibiotics, and the future effectiveness of antimicrobial agents remains in doubt [1,2]. It is imperative that a global strategy is implemented to prevent further microbial resistance, but new antimicrobial agents must also be discovered as infections with MDR-bacteria have increased to alarming levels [3]. This provides a broad requirement and rationale for expanding compound types screened against bacterial targets as part of international drug lead discovery efforts, to find new structural classes with such activities. Another threat to human life is cancer, which remains the second leading cause of mortality [4,5]. After decades of continuous effort from the scientific community, numerous achievements in the treatment and diagnosis of cancer have been achieved. However, for many cancers, a successful treatment is yet to be achieved [6]. More than 85% of all biologically-active medicinal chemical entities contain a heterocyclic component, reflecting the central role of heterocycles in modern drug design and discovery [7]. Therefore, screening new heterocyclic based compound libraries against cancer targets remains a valid approach to new drug discovery in the important arena.

Nitrogen-containing heterocyclic compounds have led to numerous promising applications in medicinal chemistry and drug discovery [8,9]. For example, quinazoline derivatives have been extensively studied for therapeutic applications against cancer [10–15]. The synthesis of several new series of imidazo[1,2-a]pyrazines related to hit compound CTN1122, an active antileishmanial, have also been reported [16–18]. Imidazo[1,2-a]pyridine derivatives have also been investigated for their anti-cancer activity in A375 and WM115 melanoma and HeLa cervical cancer cell lines [19,20]. Dibenzo[b,d]furan derivatives have also been identified as potent Pim-1/2 kinases inhibitors [21]. The pyrimidine nucleus is another significant pharmacophore at the core of drugs exhibiting excellent pharmacological activities. Numerous drugs possessing pyrimidine rings have been approved and are now commercially

* Corresponding author.
E-mail address: gardiner@manchester.ac.uk (J.M. Gardiner).
[1] Rami Y. Morjan and Ihab M. Almasri have contributed equally to this work.

https://doi.org/10.1016/j.molstruc.2023.135754
Received 10 January 2023; Received in revised form 13 April 2023; Accepted 9 May 2023
Available online 14 May 2023

available. [22]. For example, Anagliptin is an approved drug for the treatment of type 2 diabetes, while Iclaprim and Pyrazophos are important antibacterial and antifungal drugs. Benzofuro[3,2-d] pyrimidines derived from (–)cercosporamide, have also been synthesized and evaluated as potential *Candida albicans* PKC inhibitors with the aim of restoring susceptibility to azole treatment [23,24]. Recently, a benzo[e]pyrimidine emerged as a good candidate for phase I and phase II clinical trials in patients with metastatic melanoma and glioblastoma multiforme [25]. Pyrimidines have also shown activity as antitubercular, [26,27] antioxidant, [28,29] anti-inflammatory, [30,31] anticonvulsant, [32,33] antimicrobial, [34,35] antibacterial[36–38] and antitumor agents [39–44].

Herein, we describe the synthesis, docking studies, antimicrobial and anticancer activities of a series of new heterocyclic compounds 7–10 obtained through reaction of different hydrazonoyl chlorides 1–3 with substituted aminopyrimidines 4–6.(Scheme 1), proposed to proceed *via* nitrilimines generated *in situ* from hydrazonoyl chlorides 1–3 [45]. Here we report that four different heterocyclic product types furnished *via* this reaction [46–48]. Products 7 and 8 are formed through nucleophilic attack at the electrophilic carbon of the nitrilimine, via either the pyrimidine *amino* group, or of a *pyrimidine* nitrogen of 4–6, to give 7 or 8, respectively. Further cyclization of the adducts 8 can occur through pyrimidine amino group condensation with the ketone to give 9 (Scheme 1).

2. Results and Discussion

2.1. Reaction of a series of hydrazonoyl chlorides with substituted aminopyrimidines

We carried out reactions of three aminopyridines 4–6 with three hydrazonoyl chlorides 1–3. From each reaction, contrasting reactivity pathways were evident between the nitro-substituted hydrazonoyl chlorides - giving products of types 7 and /or 9, and of the *p*-Cl hydrazonoyl chloride, where high yields of the compound of type 8 were exclusively obtained.

Reaction of nitro-aryl hydrazonoyl chlorides 1 and 2 with 2-aminopyrimidine 4 gave a mixture of two products which were separated by column chromatography. The major cyclic products, imidazo[1,2-a] pyrimidine derivatives 9a and 9d, were isolated in 70% yield after recrystallization. The corresponding acyclic products 7a and 7d was also isolated as a minor product in 20% yield each.

However, when the hydrazonoyl chloride 3 was reacted with the 2-aminopyrimidine 4 (Scheme 2) under the same reaction conditions, only the acyclic product 8g was isolated in 90% yield. The structure of the products was confirmed by MS, HRMS, ^{1}H-NMR and ^{13}C-NMR (Fig. S1, Supplementary Data). Thus, the major pathway in all cases is clearly through ring nitrogen attack at the nitrilium carbon, however, in the nitro cases further condensation cyclisation is the main outcome, whilst this does not happen for the *p*-Cl derivative. In no case is any air oxidation product (10) observed. These results clearly show that the mode of the reaction and product formed are influenced by the position of the substituent group on the phenyl ring of the hydrazonoyl chlorides. The same reaction outcome was obtained in either THF or DMF. THF was preferred because the by-product, triethylamine hydrochloride, was insoluble in this solvent and was easily separated by filtration.

To investigate the mode of reaction of these reactions, and the influence of the substituent groups on the reaction pathway and time, the effect of substituent groups located on the 2-aminopyrimidine reactant was evaluated. Thus, 2-amino-4-methylpyrimidine 5 and 2-amino-4,6-dimethylpyrimidine 6, were reacted with hydrazonoyl chlorides 1-3 under the same conditions as used with 4 (*vide supra*).

The reaction of 1 with 5 produced only the cyclic imidazo[1,2-a] pyrimidine derivative 9b in 90% yield. The reaction of 2 with 5 also showed high selectivity, producing a mixture of the acyclic product 7e and the cyclic imidazo pyrimidine 9e in 10% and 80% yield respectively. So, like the part amino pyridine, this gave very high isolated yields of the product 9, with minor or no by-product isolated. In contrast, in the case of reaction of the *p*-Cl hydrazonoyl chloride 3 with 5 the acyclic adduct 8 h was the only isolated product in 90% yield (Scheme 3), mirroring the outcome seen with aminopyrdine 4, also arising from substitution using one of the pyrdimidine ring nitrogens, but without further heterocyclization.

The structure of the products confirmed by MS, HRMS, ^{1}H-NMR and ^{13}C-NMR (Fig. S2, Supplementary Data). Notable is the very different heterocyclic ring protons of compounds 8 with loss of the pyridine aromaticity, further supporting structural assignment alongside X-ray examples of compounds 7 and 9.(*vide infra*)

Next, we assessed the effect of a second methyl substituent on the pyrimidine, namely using 2-amino-4,6-dimethylpyrimidine 6. The reaction of the *o*-NO_2 derivative 1 with 6 afforded the cyclic imidazo[1,2-a]pyrimidine 9c in 70% yield, thus showing very similar selectivity to all the nitroaromatic examples above, and also produced a minor amount of the acyclic product 7c. However, under the same reaction conditions, the reaction of the *p*-NO_2 derivative 2 with 6 gave no evidence of formation of the cyclic product 9f - the major expected product from the prior nitro examples. Instead, the analogous acyclic product, 7f, was isolated in 80% purified yield. In the case of reaction of *p*-Cl derivative 3

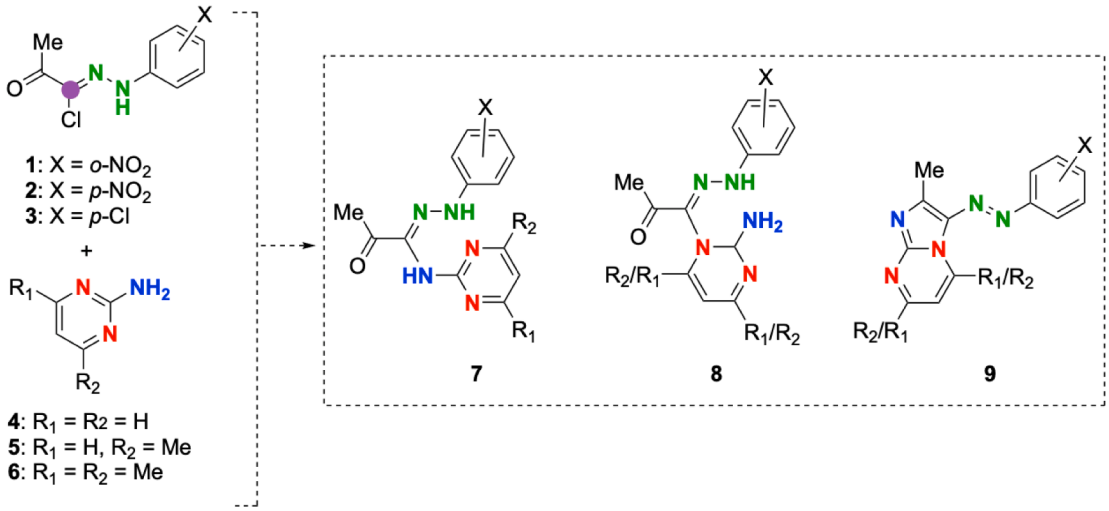

Scheme 1. Possible products from the reaction of nitrilimines 1–3 with 2-amino pyrimidine derivatives 4–6.

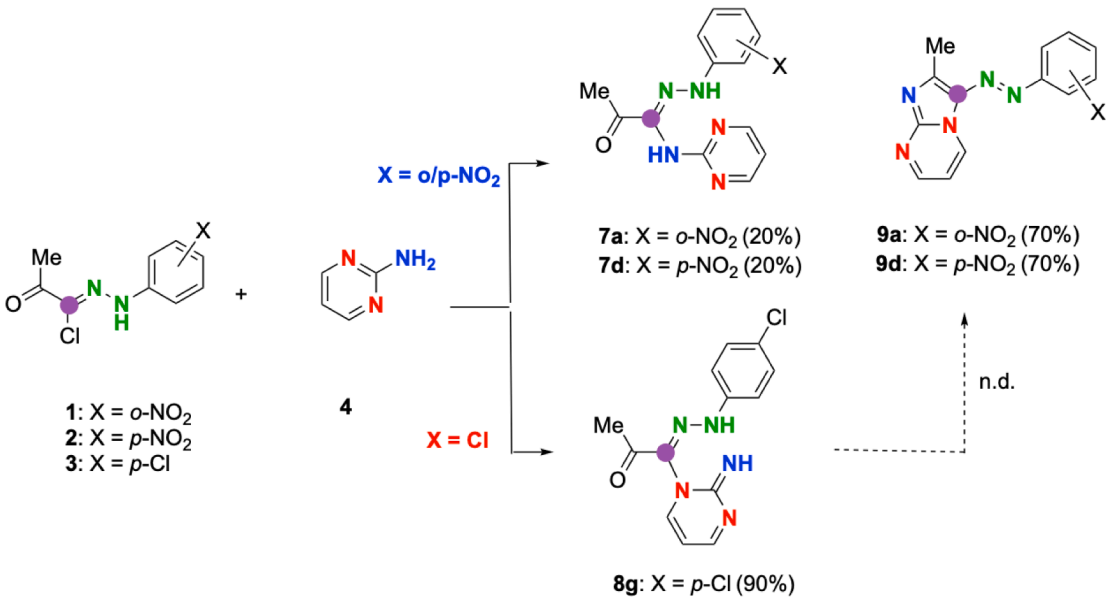

Scheme 2. Reaction of 1-3 with 2-amino pyrimidine 4.

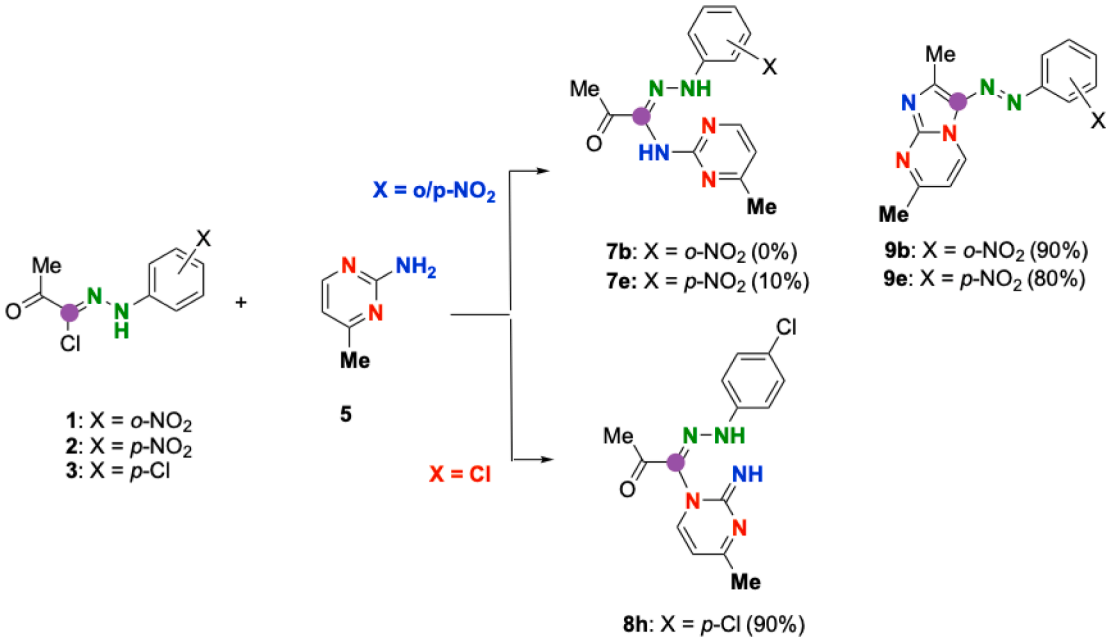

Scheme 3. Reaction of 1-3 with 2-amino-4-methylpyrimidine 5.

with 6 under the same reaction conditions; the acyclic adduct 8i was the only isolated product in 90% yield, so this again matches almost exactly the reactivity and efficiency observed for the other amino pyridines above (Scheme 4). No evidence of any by-product formation as a result of oxidation of 8i was observed [46].

2.2. X-ray structure confirmation of examples of compounds 7 and 9

The structure of the products was confirmed by MS, HRMS, ^{1}H-NMR and ^{13}C-NMR (Fig. S3, Supplementary Data), and structures of 7c and 9c were further confirmed by X-ray analyses [49]. Single crystals were obtained for both compounds on slow evaporation of 7c in DMSO/EtOH and DMSO/$CHCl_3$ for 9c. The crystal structure of compound 7c has a space point Pna 21 with a unit cell dimensions 7.321 Å, 11.762 Å, 17.508 Å and cell angles 90.00°, 90.00° and 90.00° for α, β and γ, respectively. The compound 9c has a space point group P1 with a unit cell dimensions 11.77 Å, 11.875 Å, 14.68 Å and cell angles 76.7650 (10)°, 66.7100(10)° and 63.7670(10)° for α, β and γ, respectively (Fig. 1).

The X-ray structure for compound 9c showed one oxygen atom of the NO_2 group is bonded to a molecule of $CHCl_3$. The X-ray structure for 7c indicates that the flexible N-N bond of the hydrazone exists in an anti-conformation in the crystal, while the rigid azo N=N of the linkage of 9c similarly exists in a trans configuration. Crystal packing diagrams and full details of the crystal structures are shown in (Fig. S4, Supplementary Data).

2.3. Mechanistic rationale for alternative isomer formation

The product outcomes indicate a clear preference for initial

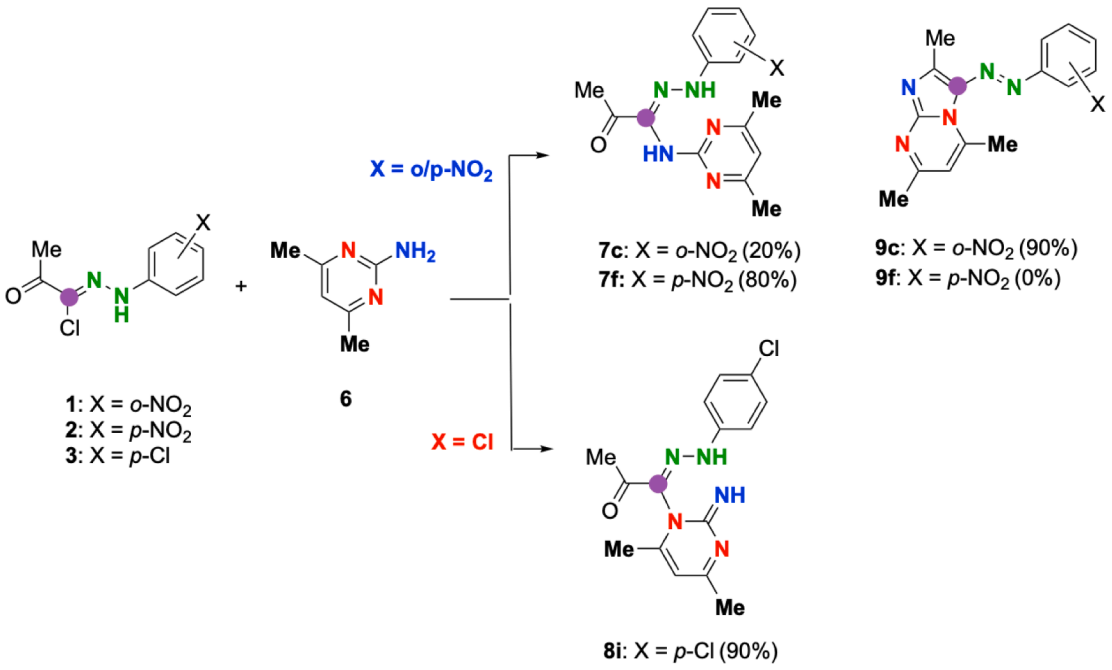

Scheme 4. Reaction of 1-3 with 2-amino-4,6-dimethylpyrimidine 6.

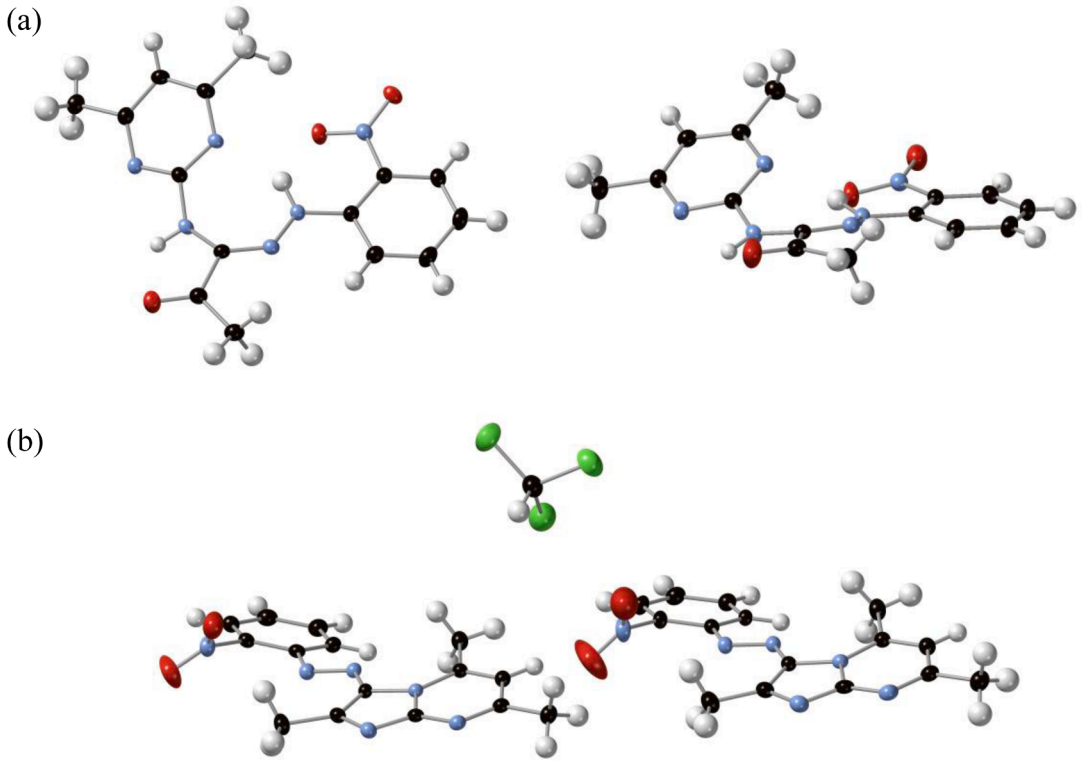

Fig. 1. (a) X-ray structures of 7c; (b) X-ray structure of 9c.

nucleophilic attach on the purported nitrimium or 1,3-diploar intermediate *via* the pyridine ring nitrogen rather than the amine group., with only one exception. This could be explained in part though hydrogen bonding interaction with a N anion, while the high regiocontrol of the outcome with unsymmetrical monomethyl pyrimidine can be rationalised through steric effects. However, this does not fully explain the preference for the *p*-Cl route to stop without conformational change and further heterocyclization (Scheme 5).

This might be accounted for by weaker activation of the carbonyl (versus nitro substituents). The only outlier to these trends is that with the dimethyl pyrimidine amino group, substitution onto the *p*-nitro hydrazonoyl chloride occurs, in similarly high yield to the isomeric outcome for the *o*-nitro hydrazonoyl chloride with this pyrimidine.

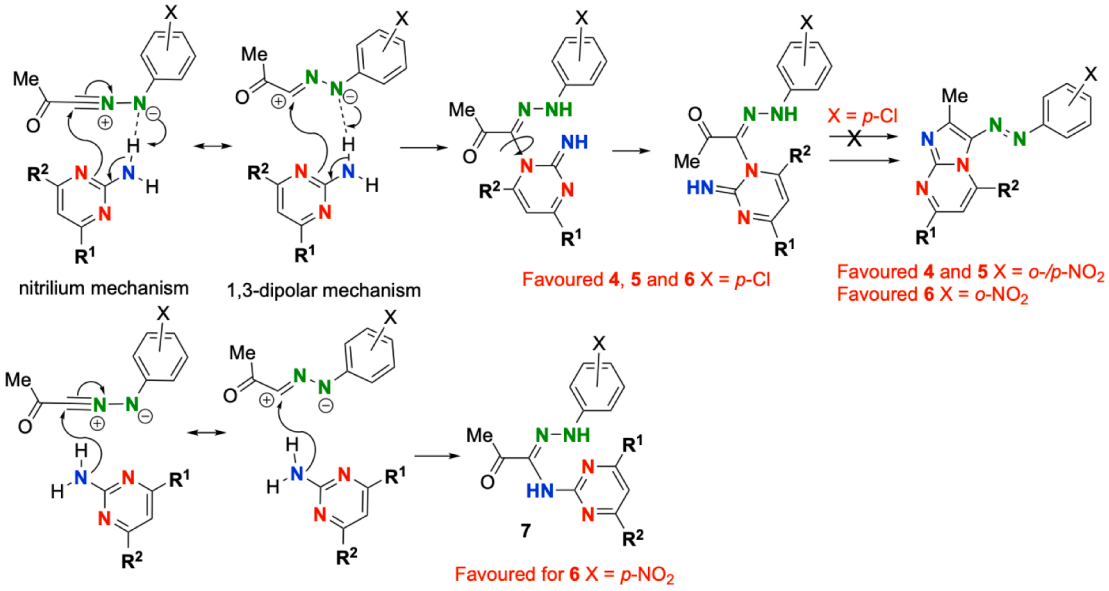

Scheme 5. Mechanism and favored outcomes for reactions of pydimidines 4-6 with hydrazonoyl chlorides 1–3.

2.4. Antibacterial evaluations

With this series of new compounds 7, 8 and 9 in hand, we then undertook evaluation of their antibacterial effects. The minimum inhibitory concentration (MIC) of the tested compounds was evaluated against six microorganisms (Two Gram-negative namely; *E. coli* ATCC 8739 and *Pseudomonas aeruginosa* ATCC 9027 and four Gram positive namely; *Staphylococcus aureus* ATCC 6538, *S. epidermidis* ATCC 12228, *Bacillus subtilis* ATCC 6633 and *Kocuria rhizophila* ATCC 9341). The microbroth dilution method was used. The obtained products were dissolved in DMSO and each test organism was grown in Brain Heart Infusion Broth (BHIB) for 4 hours [50]. The growth was adjusted to equal a 0.5 MacFarland turbidity standard. 200 µL of the adjusted growth was placed in each of 12 wells of a 96-microtiter plate [50,51]. One hundred µL of the DMSO dissolved compound was placed in the first well, mixed and 100 µL transferred to the next well. This step was repeated until the 11th well. The 12th well served as growth control. Plates were incubated for 24 h at 37 °C.

After incubation, 20 µL of 0.1% tetrazolium chloride solution was added to each well and plates were re-incubated for 15 minutes. The development of red color was indicative of bacterial growth. The lowest concentration (highest dilution) of the chemical that inhibited the growth of test organism was considered as the minimum inhibitory concentration (MIC). The screening results for antibacterial activity and determination of MIC of the synthesized compounds obtained by microdilution method showed that all compounds possessed varying degree of antibacterial activity Table 1.

However, no detectable pattern was observed and no single compound was superior to all others in terms of broader coverage and the MIC values ranged from 0.1–13.1 mg/mL. Amongst the most inhibitory results, compound 7d exhibited a MIC of 0.1 mg/mL against both *S. aureus* and *S. epidermidis* and 0.4 mg/mL against *P. aeruginosa,* whilst 7a and 9c showed MIC value of 0.2 mg/mL against *S. aureus and Kocuria rhizophila*. Most of the tested compounds reduced *P. aeruginosa* activity at concentration ≥3.2 mg/mL. The highest growth inhibition activity against *E. coli* for 8g, 7f and 7a (0.1 mg/mL). The compound 8h inhibited *E. coli* at a concentration of 0.4 mg/mL.

Table 1
The MIC results of compounds that exhibited antibacterial activity µg / mL.

	MIC in µg / mL					
	Gram-positive bacteria				Gram-negative bacteria	
Compound	*S. a*	*S.e*	*B. s*	*K.r*	*E.c*	*P.a*
7a	0.2	3.2	0.8	0.2	0.1	0.4
7c	3.2	NT	NT	3.2	3.2	3.2
7d	0.1	0.1	0.9	3.9	1.6	0.4
7f	0.8	13.1	3.2	1.6	0.1	3.2
9a	0.8	6.5	3.2	0.4	1.6	3.2
9b	1.6	6.5	6.5	0.8	0.1	3.2
9c	0.2	6.5	6.5	0.2	3.2	3.2
9d	1.6	1.6	0.2	0.8	0.2	3.2
8g	1.6	6.5	6.5	0.8	0.1	3.2
8h	0.8	0.4	0.2	0.8	0.4	3.2

[a] S. a Staphylococcus aureus ATCC 6583, S.e Staphylococcus epidermidis ATCC 12228., B.s Bacillus subtilis ATCC 6633, E.c Escherichia coli ATCC 8739, K.r. kocuria rhizophila ATCC 9341, P.a Pseudomonas aeruginosa ATCC 9027. N.T.: Not tested.

2.5. Antiproliferative effects on HeLa cells

Alongside antibacterial screening, a number of antitumor evaluations of the new compounds were undertaken.

The viability of HeLa cancer cell line was examined. The samples were first dissolved in DMSO (Sigma-Aldrich, USA) to prepare stock solutions and then diluted with complete growth medium to the final concentrations (12.5, 25, 50, 100, 200 and 400 µM) before treatment. Samples treated with DMSO alone served as controls. The final concentration of DMSO in the medium was always kept equal or less than 0.3% (v/v). Cell proliferation and viability were assessed by 3-(4,5-dimethylthiazolyl-2)-2,5-diphenyl tetrazolium bromide (MTT) (MP Biomedical, LLC, USA) assay [52]. HeLa cells were seeded at 4000 cells/well into a 96-well plate in 100 µl of complete medium. The cells were incubated for 24 h, and then exposed to various concentrations of the synthesized compounds for 24 h. At the end of the treatment, the treatment-containing medium was removed and 0.5 mg/ml MTT dissolved in the same medium was added to each well. The plate was further incubated for an additional 3 h. After removing the supernatant at the end of incubation, 100 µL DMSO was added to each well to dissolve the formazan crystals that formed. The absorbance at 570 nm was measured with a multi-well scanning spectrophotometer (Multiskan FC, USA). Cell viability was expressed as percentage of control by comparing the number of live cells in the treatment group to the number

in the vehicle group [53]. Viability of cells was calculated by the following formula:

$$\text{Viability}(\%) = \frac{\text{Mean OD of sample} - \text{OD of Blank}}{\text{Mean OD of control} - \text{OD of Blank}} \times 100$$

The results showed variable antiproliferative effects against HeLa cells (Fig. 2). The cells in the exponential growth phase were treated with eight synthesized compounds at different concentrations (12.5, 25, 50, 100, 200 and 400 μM) for 24 h. The viability of cells was determined using MTT assay where at least three independent experiments were performed. The values from each time point were then compared to the control values and expressed as mean ± SD of three or more independent experiments (Fig. S5, Supplementary Data). With the exception of 7c and 9c, the compounds inhibited the growth of HeLa cells in a dose-dependent manner ranging from 11.7 μM for 9a to 179.5 μM for 8h. The calculated IC_{50} (24 h) for the compounds which have good anti-inhibitory effect on HeLa cells are shown in Table 2.

2.6. SAR (structure activity relationship) study

The following SAR can be deduced from the anticancer screening results. Based on the obtained antiproliferative activities for the synthesized compounds listed in (Table 2); the SAR study showed that the presence of the electron donating groups (CH_3) on the pyrimidine moiety in all of the synthesized compounds listed in (Table 2) led to the decreasing of antiproliferative agent's activities. The cyclized imidazo-pyrimidine 9a,b derivatives showed the most active antiproliferative agents and, thus, higher anticancer potential activities. Moreover, incorporation of one methyl group on the pyrimidine ring within the different acyclic (series 7 and 8) and cyclic products (series 9) resulted in reduction in the activity e.g., compound 9b (IC_{50}= 90.3 μM) has about 8-fold reduction in activity in comparison to 9a (IC_{50} =11.7 μM). Similarly, compound 8h has lower activity than 8g (Table 2). Furthermore, the addition of a second methyl group on the pyrimidine ring decreased the activity substantially e.g., the activity of compound 9c (IC_{50} 4.9×10^{14} μM) dramatically decreased in comparison to compound 9a (IC_{50} 11.7 μM) and 9b (IC_{50} 90.3 μM). This is presumably due to the increase of steric hindrance which disrupted the optimum interactions between the compound and its target.

Table 2
IC_{50} (μM) (24 h) of compounds evaluated on HeLa cells.

Compound	IC_{50} (μM) (24 h)
7c	2008
7d	100.9
9a	11.7
9b	90.3
9c	4.9×10^{4}
9e	162.9
8g	80.1
8h	179.5
Taxol	1.7

2.7. Docking Simulations and Molecular Modeling

The promising antiproliferative effect of compound 9a (IC_{50} = 11.7 μM) on human cervix carcinoma HeLa cell line encouraged investigation towards proposing the potential proteins involved in the anti-proliferative effect of these compounds using an *in-silico* target fishing approach. The initial work involved Rapid overlay of chemical structures (ROCS). A database of the co-crystallized ligands was downloaded as an SDF file from Protein Data Bank (PDB; contains 217,000 entries). The database was filtered using FILTER Software in order to remove nondrug-like entities. The following parameters were adopted for filtration: allowed elements (H, C, N, O, F, P, S, Cl, Br, I); number of heavy atoms (15 to 40); molecular weight (200 to 600); number of ring system (0 to 5). The filtered PDB database had 6548 ligands. Subsequently, an ensemble of energetically accessible conformers of the target representatives (PDB database) were generated using OMEGA software with default parameters [54]. Thereafter, virtual shape/chemical matching between the designed compounds and the PDB database was carried out using ROCS software as a target fishing approach [55]. During screening, ROCS compares database compounds and query molecules by aligning the compounds such that their volumes and chemical features are as closely matched as possible. This match is represented by a TanimotoCombo score which ranges from 0 to 2. The higher the TanimotoCombo score, the better shape and chemical-feature match exists between molecules. Only antibacterial targets with ROCS score ≥ 1.0 were taken into consideration. *In silico* validation of the discovered potential targets was carried out using docking simulations. The 3D coordinates of target proteins were obtained from the Protein

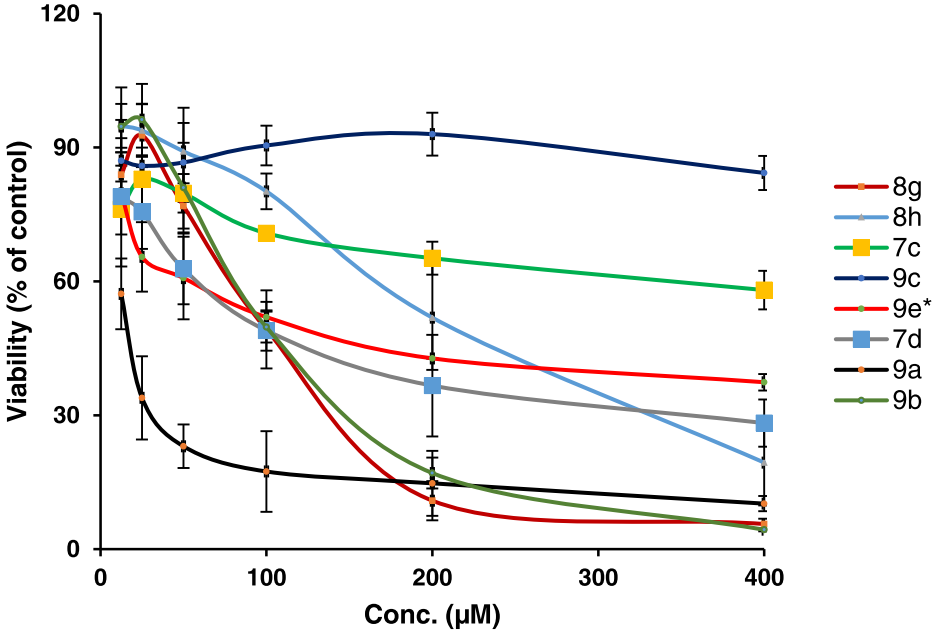

Fig. 2. Cell viability of HeLa cells with compounds 7, 8 and 9.

Data Bank. Hydrogen atoms were added to proteins using Discover Studio (DS) Visualizer templates for protein residues. The chemical structures of the designed compounds were drawn in MarvinSketch and saved in molfile format. Conformation al space for compounds was then explored by generating energetically accessible conformers using OMEGA software and the generated conformers were saved in SDF format. Subsequently, the compounds were docked into the active site of target proteins using FRED software [56] within the OEDocking suite in the presence of explicit water molecules. FRED is a fast rigid exhaustive protein-ligand docking program, which makes use of a pre-generated multiconformer database and a single receptor file as input and outputs molecules most likely to bind to the receptor [56]. The protein structures and ligand conformers are treated as rigid units during docking process. The top scoring poses are optimized and assigned a final score using Chemgauss4. Computational target profiling methods or "target fishing" are complementary to the experimental screening approaches as it is not possible to test each compound against every possible target. In order to search for potential antiproliferative targets, similarity-based target fishing approach, using ROCS program, was adopted in this work. The basic idea behind this approach is that two similar ligands are likely to have similar target-binding profiles. The fishing is carried out by using active compounds as query ligands and selecting shape and chemical similarities for comparing them with database of ligands of known bioactivities. Furthermore, to explore the capability of the designed compounds to bind to the selected targets, molecular docking simulations were used.

The results of ROCS-based target fishing revealed three potential anticancer targets of new compound 9a, ranked in the following order: Tankyrase-2 (Tank-2), Cyclin-dependent kinase (CDK2) and Epidermal growth factor tyrosine kinase receptor (EGFR).

All the designed compounds were successfully docked within the active site of the three fished targets. Tankyrases belong to a group of enzymes called poly ADP ribosyl polymerases which recently became an important novel target in treating cancer [57]. Inhibition of tankyrase catalytic activity in tumor cells prevents uncontrolled telomere extension, triggering cellular senescence and could lead to mitotic arrest without DNA damage in HeLa cells [58]. Docking simulations showed valid bonding between Tank-2 and the lead compound. A strong similarity between the binding modes of the co-crystallized ligand and the most potent designed compound 9a within the active site of Tank-2 (Figs. 3 and 4) was identified.

The nitro group and the imidazopyrimidine ring a strong network of hydrogen bonding with Ser1068, Gly1032 and Ser1033, similar to the carbonyl group and benzodioxolane ring in the co-crystallized inhibitor as shown in Fig. 3.

Fig. 3. Overlay of the highest-ranking docked pose of 9a (purple) as produced by FRED docking simulation and the co-crystallographic inhibitor of Tankyrase-2 (yellow, PDB code: 4L2K). Target structure is shown as ribbon diagram, colour-coded according to secondary structure.

Moreover, potential hydrophobic interactions could be expected with Tyr1050, Tyr1060, Tyr1071 and Ile1075. These interactions are suggested to contribute to the overall strength of the enzyme-inhibitor complex and boost the idea of considering the designed compounds as potential Tank-2 inhibitors for further investigation.

The second target, CDK2, is a serine/threonine protein kinase that plays a critical role in controlling cell proliferation through regulating the cell cycle transition from G1 to S phase. Hence, CDK2 inhibitors are considered as potentially effective anticancer agents [59]. Herein, protein-ligand docking software FRED showed similar binding profile between 9a and the co-crystallized ligand within the binding pocket of CDK2 (Figs. 5 and 6) as both compounds shown strong hydrogen bonding with the key amino acid Leu83.

Finally, EGFR is a transmembrane protein, which consists of three major functional domains: an extracellular binding domain, a hydrophobic transmembrane domain and an intracellular tyrosine kinase domain. It plays an essential role in regulating normal cell signaling, and the mutation of EGFR leads to cell proliferation, angiogenesis, invasion, metastasis and inhibition of apoptosis, accounting for the pathogenesis and progression of cancer cells. Not surprisingly, EGFR has emerged as a major target for anticancer therapeutic intervention [59]. Docking simulations showed substantial binding with good docking scores of the designed compounds against EGFR (Fig. 7). These findings could promote further studies on this target which could give rise to the discovery of new anticancer EGFR inhibitors.

3. Conclusion

Reaction of a series of hydrazonoyl chlorides 1–3 with substituted aminopyrimidines 4–6 provided chemoselective routes to new imidazo [1,2-a]pyrimidine derivatives, or regioisomeric hydrazonamide adducts. The nature of the aryl substituent in the substrate hydrazonoyl chlorides dictates the pathway, and a rationale for these selectivities is provided. Screening against a range of both gram positive and gram-negative bacteria did not establish any clear broad-spectrum lead, but did identify several compounds with MIC of 0.1-0.4 mg/mL, which offer lead targets for further development. Screening against HeLa cells also identified a new imidazo[1,2-a]pyrimidine compound (9a) which an *in silico* target fishing analysis suggests could be targeting one or more of three important cancer-treated protein targets of therapeutic interest. Modelling with these targets - Tankyrase-2 (Tank-2), Cyclin-dependent kinase (CDK2) and Epidermal growth factor tyrosine kinase receptor (EGFR) - and know ligands shows a close fit. The cell data and the modelling analysis suggest that 9a is thus a good new lead for further structure-function evaluations and ultimate mechanistic investigations targeting these three important protein targets, involving enzyme assays and structural studies.

4. Experimental section

4.1. General Experimental

^{1}H NMR spectra were recorded at 300 or 400 MHz and ^{13}C NMR spectra at 75 or 100 MHz on a Bruker AC300 or AC400 spectrometer. Chemical shifts are denoted in (ppm) relative to the internal solvent standard, TMS. ES-MS and HRMS were recorded on a Micromass LCT orthogonal acceleration time-of-flight mass spectrometer (positive and negative ion mode) with flow injection *via* a Waters 2790 separation module autosampler. Melting point determinations were made using a Stuart Scientific SMP1 apparatus and are uncorrected. All chemicals were used without further purification, as supplied by Sigma-Aldrich unless otherwise stated. The human HeLa cell line was kindly provided by Dr. Johnny Stiban (Department of Biology and Biochemistry, Birzeit University – Palestine). The cell culture media and chemicals were all purchased from Kibbutz Beit Haemek unless otherwise indicated. Cell line was routinely maintained in DMEM supplemented with

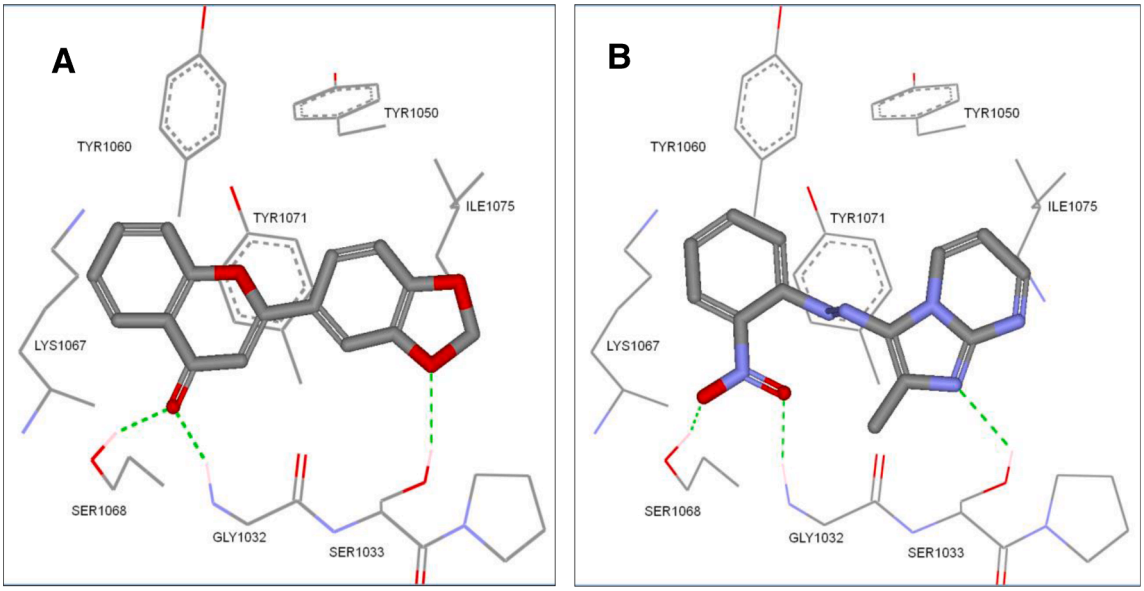

Fig. 4. Detailed view of the binding site of Tankyrase-2 (PDB code: 4L2K, Rs = 2.10 Á) showing the key interactions with (A) co-crystallized ligand (PDB code: 1V8), (B) Docked pose of compound 9a (cytotoxic IC_{50} = 11.7 μM). Green dashed-lines indicate hydrogen bonding.

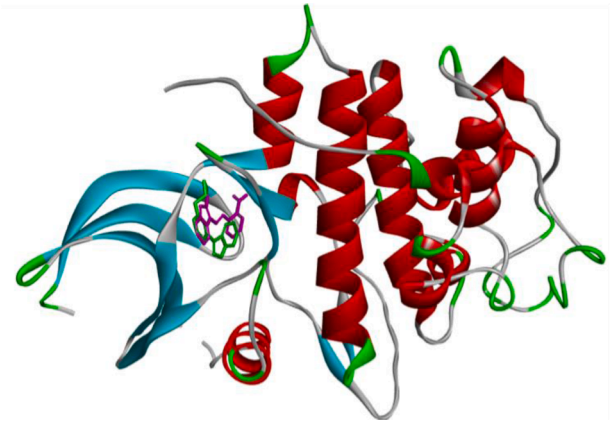

Fig. 5. Overlay of the highest-ranking docked pose of 9a (yellow) and the co-crystallized inhibitor of CDK-2 (purple, PDB code: 3EJ1). Target structure is shown as ribbon diagram, color coded according to secondary structure.

10% fetal bovine serum (FBS), 100 units/mL penicillin and 100 mg/mL streptomycin at 37 °C in a humidified 5% CO_2 air incubator

4.2. General Procedures

Triethylamine (0.01 mol, 1.4 mL) was added drop-wise at room temperature to a mixture of hydrazonoyl chloride 1–3 (0.01 mol) and the appropriate 2-aminopyrimidine derivatives 4–6 (0.012 mol) in THF (50 mL). The reaction mixture was stirred and the progress of the reaction was monitored by TLC over 24 h. The precipitated salt was filtered off and the solvent was removed in *vacuo*. The crude product was washed several times with H_2O to get rid of any remaining salt as well as any unreacted 2-aminopyrimidine derivatives. The solid was collected using suction filtration and the crude product was purified by column chromatography using 60% petroleum ether gradually changing to ethyl acetate. The following compounds were prepared according to this procedure.

4.2.1. *N'-(2-nitrophenyl)-2-oxo-N-(pyrimidin-2-yl) propanehydrazonamide 7a*

M.p. (180-182 °C); Yield (20%); ^{1}H NMR (400 MHz, $CDCl_3$) δ 12.8 (s, 1H, *o*-NO_2PhNH), 8.5 (d, *J* = 4.9 Hz, 2H, 2 x CH, pyrimidine ring), 8.4 (s, 1H, NHC=N), 8.1 (dd, *J* = 8.5, 1.5 Hz, 1H, *o*-NO_2PhCH), 7.9 (dd, *J* = 8.7, 1.2 Hz, 1H, *o*-NO_2PhCH), 7.5 (ddd, *J* = 8.6, 7.1, 1.0 Hz, 1H, *o*-NO_2PhCH), 6.9 (ddd, *J* = 8.4, 7.0, 1.3 Hz, 1H, *o*-NO_2PhCH), 6.8 (t, *J* = 4.9 Hz, 1H, CHCHCH, pyrimidine ring), 2.6 (s, 3H, CH_3CO). ^{13}C NMR (100 MHz, $CDCl_3$) δ 194.0 (C=O), 158.8 (2 x HC=N, pyrimidine ring), 158.3 (NC=N, pyrimidine ring) 140.8 (N=CCOCH$_3$), 133.5 (C-NHN), 133.3 (C-NO_2), 126.1, 119.7, 116.8, 114.4 (aromatic ring), 24.6 (CH_3C=O). LRMS (ES^+) 301 $[M + H]^+$; HRMS (TOF-ES^-) *m/z* calcd. for $C_{13}H_{13}N_6O_3[M + H]^+$ 301.1040, found 301.1044.

4.2.2. *2-Methyl-3-((2-nitrophenyl)diazenyl)imidazo[1,2-a]pyrimidine 9a*

M.p. (194–196 °C); Yield (70%); ^{1}H-NMR (400 MHz, $CDCl_3$) δ 9.8 (d, *J* = 5.9 Hz, 1H, CHCH=NC), 8.7 (dd, *J* = 4.3, 2.1 Hz, 1H), 7.9 (dd, *J* = 8.2, 1.2 Hz, 1H), 7.8 (dd, *J* = 8.1, 1.3 Hz, 1H), 7.6 – 7.5 (m, 1H), 7.4 – 7.3 (m, 1H), 7.1 (dd, *J* = 6.8, 4.3 Hz, 1H), 2.8 (s, 3H). ^{13}C-NMR (100 MHz, $CDCl_3$) δ 153.8, 149.5, 147.1, 145.5, 136.4, 133.1, 132.2, 129.3, 124.4, 117.2, 112.1, 14.3. LRMS (ES^+) 283 $[M + H]^+$; HRMS (TOF-ES^-) *m/z* calcd. for $C_{13}H_{11}N_6O_2$ $[M + H]^+$ 283.0933, found 283.0938.

4.2.3. *N-(4,6-dimethylpyrimidin-2-yl)-N'-(2-nitrophenyl)-2-oxopropanehydrazonamide 7c*

M.p. (197–199 °C); Yield (20%); ^{1}H-NMR (400 MHz, $CDCl_3$) δ 11.71 (s, 1H, *o*-NO_2PhNH), 8.11 (dd, *J* = 8.5, 1.4 Hz, 1H, *o*-NO_2PhCH), 8.08 (s, 1H, NHC=N), 7.96 (dd, *J* = 8.7, 1.1 Hz, 1H, *o*-NO_2PhCH), 7.55 (ddd, *J* = 8.1, 7.2, 0.9 Hz, 1H, *o*-NO_2PhCH), 6.90 (ddd, *J* = 8.4, 7.0, 1.3 Hz, 1H, *o*-NO_2PhCH), 6.56 (s, 1H, CH pyrimidine ring), 2.60 (s, 3H, CH_3C=O), 2.28 (s, 6H, 2 x CH_3).

^{13}C-NMR (100 MHz, $CDCl_3$) δ 194.18, 168.83, 158.32, 140.57, 135.87, 134.88, 133.35, 126.02, 119.72, 116.69, 113.61, 24.54, 23.84. LRMS (ES^+) 329 $[M + H]^+$; HRMS (TOF-ES^-) *m/z* calcd. for $C_{15}H_{17}N_6O_3$ $[M + H]^+$ 329.1357, found 329.1346.

4.2.4. *2,7-dimethyl-3-((2-nitrophenyl)diazenyl)imidazo[1,2-a]pyrimidine 9b*

M.p. (188-190 °C); Yield (90%); ^{1}H NMR (400 MHz, $CDCl_3$) δ 9.69 (d, *J* = 6.3 Hz, 1H), 7.87 (dd, *J* = 8.2, 1.1 Hz, 1H), 7.82 (dd, *J* = 8.1, 1.3 Hz,

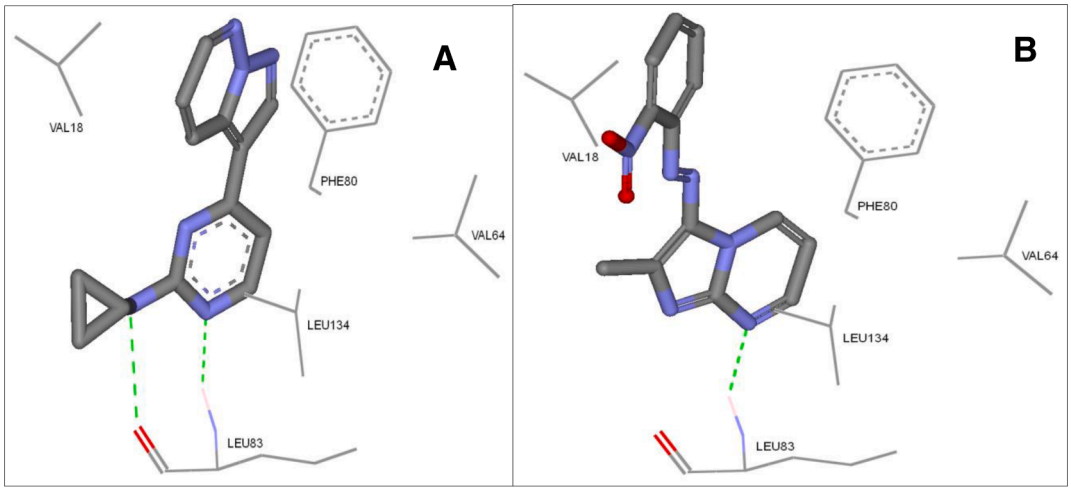

Fig. 6. Detailed view of the binding site of CDK2 (PDB code: 3EJ1, Rs = 3.22 Á) showing the key interactions with (A) co-crystallized ligand (PDB code: 5BP), (B) Docked pose of compound 9a (cytotoxic IC_{50} = 11.7 μM). Green dashed-lines indicate hydrogen bonding.

Fig. 7. Overlay of the docked pose of 9a (purple) and the co-crystallographic inhibitor of EGFR (green, PDB code: 4LL0). Target structure is shown as ribbon diagram, color-coded according to secondary structure.

1H), 7.62 – 7.52 (m, 1H), 7.43 – 7.35 (m, 1H), 6.98 (d, *J* = 6.9 Hz, 1H), 2.80 (s, 3H), 2.64 (s, 3H). ^{13}C NMR (100 MHz, $CDCl_3$) δ 165.0, 149.8, 147.0, 145.7, 135.8, 132.98, 132.02, 128.8, 124.35, 117.18, 112.68, 25.39, 14.27. LRMS (ES^+) 297 $[M + H]^+$; HRMS (TOF-ES^-) *m/z* calcd. for $C_{14}H_{13}N_6O_2$ $[M + H]^+$ 297.1086, found 297.1095.

4.2.5. 2,5,7-trimethyl-3-((2-nitrophenyl)diazenyl)imidazo[1,2-a] pyrimidine 9c

M.p. (148–150 °C); Yield (70%); ^{1}H-NMR (400 MHz, $CDCl_3$) δ 7.79 (d, *J* = 7.9 Hz, 1H, NO_2CCH), 7.63 (s, 1H, CH, nitrobenzene), 7.62 (s, 1H, CH, nitrobenzene), 7.44 (ddd, *J* = 9.8, 6.5, 4.3 Hz, 1H, CH, nitrobenzene), 6.85 (s, 1H, CH, pyrimidine ring), 3.0 (s, 3H, CH_3), 2.8 (s, 3H, CH_3), 2.7 (s, 3H, CH_3). ^{13}C-NMR (100 MHz, $CDCl_3$) δ 162.9, 150.5, 147.5, 146.4, 145.9, 144.0, 138.1, 132.3, 128.6, 123.8, 117.1, 113.0, 24.7, 21.7, 18.7. LRMS (ES^+) 311 $[M + H]^+$; HRMS (TOF-ES^-) *m/z* calcd. for $C_{15}H_{15}N_6O_2$ $[M + H]^+$ 311.1258, found 311.1241.

4.2.6. 1-(2-(4-chlorophenyl)hydrazono)-1-(2-iminopyrimidin-1(2H)-yl) propan-2-one 8g

M.p. (191–192 °C); Yield (90%); ^{1}H NMR (400 MHz, DMSO) δ 8.7 (d, *J* = 10.8 Hz, 1H, CH, pyrimidine ring), 8.0 (d, *J* = 8.9 Hz, 2H, *p*-ClPhCH), 7.8 (s, 1H, NH), 7.7 (d, *J* = 12.7 Hz, 1H, CH, pyrimidine ring), 7.6 (d, *J* = 8.9 Hz, 2H, *p*-ClPhCH), 5.6 (dd, *J* = 11.7, 11.2 Hz, 1H, CH, pyrimidine ring), 3.4 (s, 3H, CH_3). ^{13}C-NMR (100 MHz, DMSO) δ 191.1, 168.9, 160.9, 160.4, 157.1, 136.3, 131.5, 128.9, 124.5, 101.0, 26.8. LRMS (ES^+) 290 $[M + H]^+$; HRMS (TOF-ES^-) *m/z* calcd. for $C_{13}H_{13}ClN_5O$ $[M + H]^+$ 290.0739, found 290.0809.

4.2.7. 1-(2-(4-chlorophenyl)hydrazono)-1-(2-imino-6-methylpyrimidin-1 (2H)-yl)propan-2-one 8h

M.p. (196–198 °C); Yield (90%); ^{1}H-NMR (400 MHz, $CDCl_3$) δ 9.2 (s, 1H, NH, *p*-ClPhNH), 7.6 (d, *J* = 8.9 Hz, 2H, *p*-ClPhCH), 7.4 (d, *J* = 8.9 Hz, 2H, *p*-ClPhCH),6.8– 6.7 (m, 1H, CH=N, pyrimidine ring), 5.1 (s, 1H, NHC=N), 4.8 (d, *J* = 7.8 Hz, 1H, CH=C, pyrimidine ring), 2.6 (s, 3H, CH_3C=O), 2.3 (s, 3H, CH_3). ^{13}C NMR (100 MHz, $CDCl_3$) δ 192.7 (CH_3C=O), 177.3, 158.1, 157.6, 147.7, 136.2, 133.8, 129.1, 125.0, 97.3, 77.3, 77.0, 76.7, 26.8, 24.2. LRMS (ES^+) 304 $[M + H]^+$; HRMS (TOF-ES^-) *m/z* calcd. for $C_{14}H_{15}$ ClN_5O $[M + H]^+$ 304.0966, found 304.0950.

4.2.8. 1-(2-(4-chlorophenyl)hydrazono)-1-(2-imino-4,6-dimethylpyrimidin-1(2H)-yl)propan-2-one 8i

M.p. (207–209 °C); Yield (90%); ^{1}H NMR (400 MHz, $CDCl_3$) δ 11.9 (s, 1H, s, 1H, NH, *p*-ClPhNH), 8.3 (s, 1H,CH_3C=CHC=N), 7.3 (d, *J* = 8.9 Hz, 2H, *p*-ClPhCH), 7.1 (d, *J* = 8.9 Hz, 2H, *p*-ClPhCH), 6.6 (s, 1H, s, 1H, NHC=N), 2.6 (s, 3H, CH_3C=O), 2.4 (s, 6H, 2x CH_3). ^{13}C NMR (100 MHz, $CDCl_3$) δ 193.4 (CH_3C=O), 168.3, 143.3, 131.6, 129.3, 129.2, 125.9, 115.1, 114.8, 112.5, 24.2, 23.8, 23.3.

4.2.9. N'-(4-nitrophenyl)-2-oxo-N-(pyrimidin-2-yl) propanehydrazonamide 7d

M.p. (168–170 °C); Yield (20%); ^{1}H-NMR (400 MHz, $CDCl_3$) δ 12.4 (s, 1H, *p*-NO_2PhNH), 8.5 (s, 1H, NHC=N), 8.4 (d, *J* = 4.9 Hz, 2H, pyrimidine ring), 8.2 (d, *J* = 9.3 Hz, 2H, *p*-NO_2PhCH), 7.1 (d, *J* = 9.1 Hz, 2H, *p*-NO_2PhCH), 6.8 (t, *J* = 4.9 Hz, 1H, pyrimidine ring), 2.6 (s, 3H, CH_3C=O). ^{13}C-NMR (100 MHz, $CDCl_3$) δ 164.0 (C=O), 156.9 (2 x HC=N, pyrimidine ring), 154.1 (NC=N, pyrimidine ring) 140.8 (N=$CCOCH_3$), 133.5 (C-NHN), 133.3 (C-NO_2), 125.3, 124.5, 122.6, 112.5 (aromatic ring), 14.4 (CH_3C=O) LRMS (ES^+) 301 $[M + H]^+$; HRMS (TOF-ES^-) *m/z* calcd. for $C_{13}H_{13}N_6O_3$ $[M + H]^+$ 301.1040, found 301.1044. LRMS (ES^+) 301 $[M + H]^+$.

4.2.10. 2-Methyl-3-((4-nitrophenyl)diazenyl)imidazo[1,2-a]pyrimidine 9d

M.p. (200-201 °C); Yield (70%); ^{1}H NMR (400 MHz, $CDCl_3$) δ 9.96 (d, J = 3.1 Hz, 1H), 8.71 (dd, J = 4.3, 2.1 Hz, 1H), 8.29 (d, J = 9.0 Hz, 2H), 7.90 (d, J = 9.0 Hz, 2H), 7.14 (dd, J = 6.8, 4.3 Hz, 1H), 2.86 (s, 3H). ^{13}C NMR (100 MHz, $CDCl_3$) δ 156.9, 153.6, 149.4, 147.5, 136.1, 131.1, 124.9, 122.2, 111.8, 14.4. LRMS (ES^+) 283 $[M + H]^+$; HRMS (TOF-ES^-) m/z calcd. for $C_{13}H_{11}N_6O_2$ $[M + H]^+$ 283.0933, found 283.0938.

4.2.11. N-(4-Methylpyrimidin-2-yl)-N'-(4-nitrophenyl)-2-oxopropanehydrazonamide 7e

M.p. (197–199 °C); Yield (10%); ^{1}H NMR (400 MHz, $CDCl_3$) δ 12.73 (s, 1H, NH, p-NO_2PhNH), 8.48 (s, 1H, NHC=N), 8.27 (d, J = 5.1 Hz, 1H, pyrimidine ring), 8.16 (d, J = 9.2 Hz, 2H, p-NO_2PhNH), 7.12 (d, J = 9.1 Hz, 2H, p-NO_2PhNH), 2.58 (s, 3H, CH_3C=O), 2.44 (s, 3H, CH_3). LRMS (ES^-) 313 $[M - H]^+$.

4.2.12. 2,7-dimethyl-3-((4-nitrophenyl)diazenyl)imidazo[1,2-a]pyrimidine 9e

M.p. (211–213 °C); Yield (80%); ^{1}H NMR (400 MHz, $CDCl_3$) δ 9.80 (d, J = 1.5 Hz, 1H), 8.28 (d, J = 9.1 Hz, 2H), 7.87 (d, J = 9.1 Hz, 2H), 6.98 (d, J = 6.9 Hz, 1H), 2.81 (s, 3H), 2.66 (s, 3H). LRMS (ES^+) 297 $[M + H]^+$; HRMS (TOF-ES^-) m/z calcd. for $C_{14}H_{13}N_6O_2[M + H]^+$ 297.1095, found 297.1092.

4.2.13. N-(4,6-Dimethylpyrimidin-2-yl)-N'-(4-nitrophenyl)-2-oxopropanehydrazonamide 7f

M.p. (200–202 °C); Yield (80%); ^{1}H NMR (400 MHz, $CDCl_3$) δ 13.13 (s, 1H, p-NO_2PhNH), 8.52 (s, 1H, NHC=N), 8.23 (d, J = 9.2 Hz, 2H, p-NO_2PhCH), 7.20 (d, J = 9.1 Hz, 2H, p-NO_2PhCH CH), 6.65 (s, 1H, Pyrimidine ring), 2.65 (s, 3H, CH_3C=O), 2.46 (s, 6H, 2 x CH_3).

^{13}C NMR (100 MHz, $CDCl_3$) δ 193.4, 168.4, 158.0, 149.6, 140.8, 132.7, 126.2, 113.2, 112.5, 77.4, 77.0, 76.7, 24.3, 23.8. LRMS (ES^+) 329 $[M + H]^+$; HRMS (TOF-ES^-) m/z calcd. for $C_{15}H_{17}N_6O_3$ $[M + H]^+$ 329.1357, found 329.1346.

Associated content

Supporting material including ^{1}H, ^{13}C, NMR spectra, is available free of charge via the internet, in the online version.

CRediT authorship contribution statement

Rami Y. Morjan: Investigation, Data curation, Writing – review & editing, Writing – original draft. **Amany F. El-Hallaq:** Investigation, Data curation, Writing – review & editing, Writing – original draft. **Jannat N. Azarah:** Investigation, Data curation, Writing – review & editing, Writing – original draft. **Ihab M. Almasri:** Investigation, Data curation, Writing – review & editing, Writing – original draft. **Mazen M. Alzaharna:** Investigation, Data curation, Writing – review & editing, Writing – original draft. **Mariam R. Al-Reefi:** Investigation, Data curation, Writing – review & editing, Writing – original draft. **Ian Beadham:** Investigation, Data curation, Writing – review & editing, Writing – original draft. **Omar S. Abu-Teim:** Investigation, Data curation, Writing – review & editing, Writing – original draft. **Abdelraouf A. Elmanama:** Investigation, Data curation, Writing – review & editing, Writing – original draft. **Adel M. Awadallah:** Investigation, Data curation, Writing – review & editing, Writing – original draft. **James Raftery:** Investigation, Data curation, Writing – review & editing, Writing – original draft. **John M. Gardiner:** Investigation, Data curation, Writing – review & editing, Writing – original draft.

Declaration of Competing Interest

The authors declare that they have no known competing financial interests or personal relationships that could have appeared to influence the work reported in this paper.

Data availability

Further data supporting this work is included in the SI.

Acknowledgment

This work was supported by The World Academy of Sciences for the Advancement of Science in Developing Countries (TWAS) through financial support to A. M. Awadallah, R. Y. Morjan, I. M. Almasri and M. M. Alzaharna (grant no. 16-490-RG/CHE/AF/AC_G-FR3240293296) and to J. N. Azarah (Scholarship no. 16-490 RG/CHE/AF/AC_G-FR3240293296). EPSRC for NMR instrumention grant EP/K039547/1 supported NMR data in this paper.

Supplementary materials

Supplementary material associated with this article can be found, in the online version, at doi:10.1016/j.molstruc.2023.135754.

References

[1] M. Terreni, M. Taccani, M. Pregnolato, New antibiotics for multidrug-resistant bacterial strains: latest research developments and future perspectives, Molecules 26 (2021) 2671, https://doi.org/10.3390/molecules26092671.
[2] M.A. Fischbach, T.C. Walsh, Antibiotics for emerging pathogens, Science 325 (2009) 1089, https://doi.org/10.1126/science.1176667.
[3] R. Morjan, A. Mkadmh, I. Beadham, A. Elmanama, M. Mattar, J. Raftery, R. Pritchard, A. Awadallah, J. Gardiner, Antibacterial activities of novel nicotinic acid hydrazides and their conversion into N-acetyl-1, 3, 4-oxadiazoles, Bioorg. Med. Chem. Lett. 24 (2014) 5796–5800, https://doi.org/10.1016/j.bmcl.2014.10.029.
[4] H. Nagai, Y.H. Kim, Cancer prevention from the perspective of global cancer burden patterns, J. Thorac. Dis. 9 (2017) 448–451, https://doi.org/10.21037/jtd.2017.02.75.
[5] M. Krause, H. Foks, K. Gobis, Pharmacological potential and synthetic approaches of imidazo[4,5-b]pyridine and imidazo[4,5-c]pyridine derivatives, Molecules 22 (2017) 399, https://doi.org/10.3390/molecules22030399.
[6] F. Biemar, M. Foti, Global progress against cancer-challenges and opportunities, Cancer Biol. Med. 10 (2013) 183–186, https://doi.org/10.7497/j.issn.2095-3941.2013.04.001.
[7] M.M. Heravi, V. Zadsirjan, Prescribed drugs containing nitrogen heterocycles: an overview, RSC Adv. 10 (2020) 44247–44311, https://doi.org/10.1039/D0RA09198G.
[8] É. Frank, G. Szőllősi, Nitrogen-containing heterocycles as significant molecular scaffolds for medicinal and other applications, Molecules 26 (2021) 4617, https://doi.org/10.3390/molecules26154617.
[9] J. Jampilek, Heterocycles in medicinal chemistry, Molecules 24 (2019) 3839, https://doi.org/10.3390/molecules24213839.
[10] P. Wdowiak, J. Matysiak, P. Kuszta, K. Czarnek, E. Niezabitowska, T. Baj, Quinazoline derivatives as potential therapeutic agents in urinary bladder cancer therapy, Front. Chem. 9 (2021) 1–14, https://doi.org/10.3389/fchem.2021.765552.
[11] Li Y., Xiao J., Zhang Q., Yu W., Liu M., Guo Y., He J., Liu Y., The association between anti-tumor potency and structure-activity of protein-kinases inhibitors based on quinazoline molecular skeleton (2018), (1464-3391 (Electronic)). 10.1016/j.bmc.2018.12.032.
[12] D. Das, J. &Hong, Recent advancements of 4-aminoquinazoline derivatives as kinase inhibitors and their applications in medicinal chemistry, Eur. J. Med. Chem. 170 (2019) 55–72, https://doi.org/10.1016/j.ejmech.2019.03.004.
[13] S. Kasibhatla, V. Baichwal, S.X. Cai, B. Roth, I. Skvortsova, S. Skvortsov, P. Lukas, N.M. English, N. Sirisoma, J. Drewe, A. Pervin, B. Tseng, R.O. Carlson, C. M. Pleiman, MPC-6827: a small-molecule inhibitor of microtubule formation that is not a substrate for multidrug resistance pumps, Cancer Res. 67 (2007) 5865–5871, https://doi.org/10.1158/0008-5472.CAN-07-0127.
[14] N. Sirisoma, S. Kasibhatla, A. Pervin, H. Zhang, S. Jiang, J.A. Willardsen, M. B. Anderson, V. Baichwal, G.G. Mather, K. Jessing, R. Hussain, K. Hoang, C. M. Pleiman, B. Tseng, J. Drewe, S.X. Cai, Discovery of 2-Chloro-N-(4-methoxy-phenyl)-N-methylquinazolin-4-amine (EP128265, MPI-0441138) as a Potent inducer of apoptosis with high *in vivo* activity, J. Med. Chem. 51 (2008) 4771–4779, https://doi.org/10.1021/jm8003653.
[15] Oyallon B., Brachet-Botineau M., Logé C.A.O., Robert T., Bach S.A.O., Ibrahim S.A. O., Raoul W.A.O., Croix C., Berthelot P., Guillon J.A.O., Pinaud N.A.O., Gouilleux F.A.O., Viaud-Massuard M.C., Denevault-Sabourin C., New quinoxaline derivatives as dual pim-1/2 kinase inhibitors: design, synthesis and biological evaluation. (2021). 10.3390/molecules26040867.

[16] M.A. Bazin, S. Cojean, F. Pagniez, G. Bernadat, C. Cavé, I. Ourliac-Garnier, M. R. Nourrisson, C. Morgado, C. Picot, O. Leclercq, B. Baratte, T. Robert, G.F. Späth, N. Rachidi, S. Bach, P.M. Loiseau, P. Le Pape, P. Marchand, *In vitro* identification of imidazo[1,2-a]pyrazine-based antileishmanial agents and evaluation of L. major casein kinase 1 inhibition, Eur. J. Med. Chem. 210 (2021), 112956, https://doi.org/10.1016/j.ejmech.2020.112956.

[17] P. Marchand, M.A. Bazin, F. Pagniez, G. Rivière, L. Bodero, S. Marhadour, M. R. Nourrisson, C. Picot, S. Ruchaud, S. Bach, B. Baratte, M. Sauvain, D.C. Pareja, A. J. Vaisberg, P. Le Pape, Synthesis, antileishmanial activity and cytotoxicity of 2,3-diaryl- and 2,3,8-trisubstituted imidazo[1,2-a]pyrazines, Eur. J. Med. Chem. 103 (2015) 381–395, https://doi.org/10.1016/j.ejmech.2015.09.002.

[18] S. Marhadour, P. Marchand, F. Pagniez, M.A. Bazin, C. Picot, O. Lozach, S. Ruchaud, M. Antoine, L. Meijer, N. Rachidi, P. Le Pape, Synthesis and biological evaluation of 2,3-diarylimidazo[1,2-a]pyridines as antileishmanial agents, Eur. J. Med. Chem. 58 (2012) 543–556, https://doi.org/10.1016/j.ejmech.2012.10.048.

[19] S. Aliwaini, A.M. Awadallah, R.Y. Morjan, M. Ghunaim, H. Alqaddi, A. Y. Abuhamad, E.A. Awadallah, Y.M. Abughefra, Novel imidazo[1,2a]pyridine inhibits AKT/mTOR pathway and induces cell cycle arrest and apoptosis in melanoma and cervical cancer cells, Oncol. Lett. 18 (2019) 830–837, https://doi.org/10.3892/ol.2019.10341.

[20] J. Wang, H. Wu, G. Song, D. Yang, J. Huang, X. Yao, H. Qin, Z. Chen, Z. Xu, C. Xu, A novel imidazopyridine derivative exerts anticancer activity by inducing mitochondrial pathway-mediated apoptosis, BioMed. Res. Int. 2020 (2020), 4929053, https://doi.org/10.1155/2020/4929053.

[21] V.H. Dao, I. Ourliac-Garnier, C. Logé, F.O. McCarthy, S. Bach, T.G. da Silva, C. Denevault-Sabourin, J. Thiéfaine, B. Baratte, T. Robert, F. Gouilleux, M. Brachet-Botineau, M.-A. Bazin, P. Marchand, Dibenzofuran derivatives inspired from cercosporamide as dual inhibitors of Pim and CLK1 kinases, Molecules 26 (2021) 6572, https://doi.org/10.3390/molecules26216572.

[22] V. Sharma, N. Chitranshi, A.K. Agarwal, Significance and biological importance of pyrimidine in the microbial world, Int. J. Med. Chem. 2014 (2014) 1–31, https://doi.org/10.1155/2014/202784.

[23] V.H. Dao, I. Ourliac-Garnier, M.-A. Bazin, C. Jacquot, B. Baratte, S. Ruchaud, S. Bach, O. Grovel, P. Le Pape, P. Marchand, Benzofuro[3,2-d]pyrimidines inspired from cercosporamide CaPkc1 inhibitor: synthesis and evaluation of fluconazole susceptibility restoration, Bioorg. Med. Chem. Lett. 28 (2018) 2250–2255, https://doi.org/10.1016/j.bmcl.2018.05.044.

[24] A. Sussman, K. Huss, L.C. Chio, S. Heidler, M. Shaw, D. Ma, G. Zhu, R.M. Campbell, T.S. Park, P. Kulanthaivel, J.E. Scott, J.W. Carpenter, M.A. Strege, M.D. Belvo, J. R. Swartling, A. Fischl, W.K. Yeh, C. Shih, X.S. Ye, Discovery of cercosporamide, a known antifungal natural product, as a selective Pkc1 kinase inhibitor through high-throughput screening, Eukaryot. Cell 3 (2004) 932–943, https://doi.org/10.1128/EC.3.4.932-943.2004.

[25] Y. Loidreau, M.-R. Nourrisson, C. Fruit, C. Corbière, P. Marchand, T. Besson, Microwave-Assisted Synthesis of Potential Bioactive Benzo-, Pyrido- or Pyrazino-thieno[3,2-d]pyrimidin-4-amine Analogs of MPC-6827, Pharmaceuticals (Basel) 13 (2020) 202, https://doi.org/10.3390/ph13090202.

[26] P. Liu, Y. Yang, Y. Tang, T. Yang, Z. Sang, Z. Liu, T. Zhang, Y. Luo, Design and synthesis of novel pyrimidine derivatives as potent antitubercular agents, Eur. J. Med. Chem. 163 (2019) 169–182, https://doi.org/10.1016/j.ejmech.2018.11.054.

[27] I. Kostova, Y.P. Atanasov, Antioxidant Properties of Pyrimidine and Uracil Derivatives, Curr. Org. Chem. 21 (2017) 2096–2108, https://doi.org/10.2174/1385272820666161025152154.

[28] S. Khajeh Dangolani, F. Panahi, Z. Tavaf, M. Nourisefat, R. Yousefi, A. Khalafi-Nezhad, Synthesis and antioxidant activity evaluation of some novel aminocarbonitrile derivatives incorporating carbohydrate moieties, ACS Omega 3 (2018) 10341–10350, https://doi.org/10.1021/acsomega.8b01124.

[29] H.U. Rashid, M.A.U. Martines, A.P. Duarte, J. Jorge, S. Rasool, R. Muhammad, N. Ahmad, M.N. Umar, Research developments in the syntheses, anti-inflammatory activities and structure–activity relationships of pyrimidines, RSC Adv. 11 (2021) 6060–6098, https://doi.org/10.1039/D0RA10657G.

[30] S. Kumar, B. Narasimhan, Therapeutic potential of heterocyclic pyrimidine scaffolds, Chem. Cent. J. 12 (2018) 38, https://doi.org/10.1186/s13065-018-0406-5.

[31] R.G. Paronikyan, Novel pyrimidine derivatives with anticonvulsant and psychotropic effects, Epilepsy Paroxysmal Cond. 9 (2017) 39–46, https://doi.org/10.17749/2077-8333.2017.9.3.040-046.

[32] H.J. Zhang, S.B. Wang, X. Wen, J.Z. Li, Z.S. Quan, Design, synthesis, and evaluation of the anticonvulsant and antidepressant activities of pyrido[2,3-d]pyrimidine derivatives, Med. Chem. Res. 25 (2016) 1287–1298, https://doi.org/10.1007/s00044-016-1559-1.

[33] J. Zhuang, S. Ma, Recent Development of pyrimidine-containing antimicrobial agents, ChemMedChem 15 (2020) 1875–1886, https://doi.org/10.1002/cmdc.202000378.

[34] Y. Luo, S. Zhang, Z.J. Liu, W. Chen, J. Fu, Q.F. Zeng, H.L. Zhu, Synthesis and antimicrobical evaluation of a novel class of 1,3,4-thiadiazole: Derivatives bearing 1,2,4-triazolo[1,5-a]pyrimidine moiety, Eur. J. Med. Chem. 64 (2013) 54–61, https://doi.org/10.1016/j.ejmech.2013.04.014.

[35] M. Horchani, A. Hajlaoui, A.H. Harrath, L. Mansour, H. Ben Jannet, A. Romdhane, New pyrazolo-triazolo-pyrimidine derivatives as antibacterial agents: design and synthesis, molecular docking and DFT studies, J. Mol. Struct. 1199 (2020), 127007, https://doi.org/10.1016/j.molstruc.2019.127007.

[36] M. Ahmed, M. Sayed, A.F. Saber, R. Hassanien, A.M. Kamal El-Dean, M.S. Tolba, Synthesis, characterization, and antimicrobial activity of new thienopyrimidine derivatives, Polycycl. Aromat. Compd. 42 (2020) 3079–3088, https://doi.org/10.1080/10406638.2020.1852587.

[37] Y. Rival, G. Grassy, G. Michel, Synthesis and antibacterial activity of some imidazo [1, 2-α]pyrimidine derivatives, Chem. Pharm. Bull. 40 (1992) 1170–1176, https://doi.org/10.1248/cpb.40.1170.

[38] B. Tylińska, B. Wiatrak, Ż. Czyżnikowska, A. Cieśla-Niechwiadowicz, E. Gębarowska, A. Janicka-Kłos, Novel pyrimidine derivatives as potential anticancer agents: synthesis, biological evaluation and molecular docking study, Int. J. Mol. Sci. 22 (2021) 3825, https://doi.org/10.3390/ijms22083825.

[39] Z. Kilic-Kurt, N. Ozmen, F. Bakar-Ates, Synthesis and anticancer activity of some pyrimidine derivatives with aryl urea moieties as apoptosis-inducing agents, Bioorg. Chem. 101 (2020), 104028, https://doi.org/10.1016/j.bioorg.2020.104028.

[40] N.M. Ahmed, M.M. Youns, M.K. Soltan, A.M. Said, Design, synthesis, molecular modeling and antitumor evaluation of novel indolyl-pyrimidine derivatives with egfr inhibitory activity, Molecules 26 (2021) 1838, https://doi.org/10.3390/molecules26071838.

[41] Y. Loidreau, C. Dubouilh-Benard, M.-R. Nourrisson, N. Loaëc, L. Meijer, T. Besson, P. Marchand, Exploring kinase inhibition properties of 9H-pyrimido[5,4-b]- and [4,5-b]indol-4-amine derivatives, Pharmaceuticals 13 (2020), https://doi.org/10.3390/ph13050089.

[42] A.R. Sayed, S.M. Gomha, Y.S. Al-Faiyz, Y.H. Zaki, New Convenient routes of hydrazonoyl halides for the synthesis of novel thiazoles and polythiazoles, Polycycl. Aromat. Compd. 42 (2020) 3318–3327, https://doi.org/10.1080/10406638.2020.1866032.

[43] A.S. Shawali, A review on bis-hydrazonoyl halides: recent advances in their synthesis and their diverse synthetic applications leading to bis-heterocycles of biological interest, J. Adv. Res. 7 (2016) 873–907, https://doi.org/10.1016/j.jare.2016.09.001.

[44] Q. Zhang, S. Chen, X. Liu, W. Lin, K. Zhu, Equisetin restores colistin sensitivity against multi-drug resistant gram-negative bacteria, Antibiotics 10 (2021) 1263, https://doi.org/10.3390/antibiotics10101263.

[45] R.Y. Morjan, B. Qeshta, H.T. Al-Shayyah, J.M. Gardiner, B.A. Abu Thaher, A. M. Awadallah, Reaction of nitrilimines with 2-aminopicoline, 3-amino-1, 2, 4-triazole, 5-aminotetrazole and 2-aminopyrimidine, Int. J. Org. Chem. 4 (2014) 201–207, https://doi.org/10.4236/ijoc.2014.43023.

[46] A.M. Awadallah, J.A. Zahra, Reaction of nitrilimines with 2-substituted Aza-heterocycles. synthesis of pyrrolo[1,2-a]pyridine and Pyrimido[2,1-d]1,2,3,5-tetrazine, Molecules 13 (2008) 170–176, https://doi.org/10.3390/molecules13010170.

[47] A.S. Shawali, A.A. Elghandour, S.M. El-Sheikh, A new one-step synthesis of pyrimido-[1,2-b][1,2,4,5]tetrazines, Heteroatom Chem. 11 (2000) 87–90, https://doi.org/10.1002/(SICI)1098-1071(2000)11:2.

[48] N.A. Hassan, Two-component, one-pot synthesis of pyrimido[1,2-b] [1,2,4,5] tetrazines, J. Sulfur Chem. 27 (2006) 605–615, https://doi.org/10.1080/17415990601039584.

[49] Cambridge crystallographic data centre for small molecules CCDC for compound 7c (1519135) and for 9c (1519134). (2023).

[50] A. Elmanama, M. Al-Reefi, Antimicrobial, anti-biofilm, anti-quorum sensing, antifungal and synergistic effects of some medicinal plants extract, IUG J. Nat. Engl.Stud. 25 (2017) 198–207.

[51] R.Y. Morjan, F.J. Ghonium, J.N. Azarah, O.S. Abu-Teim, A.M. Awadallah, M.R. Al-Reefi, A.A. Elmanama, J.M. Gardiner, Syntheses of N-acylhydrazones of 2-hydroxy-3, 5-dinitrobenzohydrazide, and their Conversion into 3-Acetyl-2, 3-dihydro-1, 3, 4-oxadiazole, IUG J. Nat. Stud. 30 (2022) 38–46, https://doi.org/10.33976/IUGNS.30.2/2022/4.

[52] Weinstein M.P., Lewis J.S., 2nd, The clinical and laboratory standards institute subcommittee on antimicrobial susceptibility testing: background, organization, functions, and processes. (2020) LID - 10.1128/JCM.01864-19 [doi] LID - e01864-19, (1098-660X (Electronic)). 10.1128/JCM.01864-19.

[53] M. Alzaharna, I. Alqouqa, H.Y. Cheung, Taxifolin synergizes Andrographolide-induced cell death by attenuation of autophagy and augmentation of caspase dependent and independent cell death in HeLa cells, PLoS One 12 (2017), e0171325, https://doi.org/10.1371/journal.pone.0171325.

[54] P.C.D. Hawkins, A.G. Skillman, G.L. Warren, B.A. Ellingson, M.T. Stahl, Conformer generation with OMEGA: algorithm and validation using high quality structures from the protein databank and cambridge structural database, J. Chem. Inf. Model. 50 (2010) 572–584, https://doi.org/10.1021/ci100031x.

[55] P.C.D. Hawkins, A.G. Skillman, A. Nicholls, Comparison of shape-matching and docking as virtual screening tools, J. Med. Chem. 50 (2007) 74–82, https://doi.org/10.1021/jm0603365.

[56] M. McGann, FRED and HYBRID docking performance on standardized datasets, J. Comput. Aided Mol. Des. 26 (2012) 897–906, https://doi.org/10.1007/s10822-012-9584-8.

[57] V.T. Lakshmi, S. Bale, A. Khurana, C. Godugu, Tankyrase as a novel molecular target in cancer and fibrotic diseases, Curr. Drug Targets 18 (2017) 1214–1224, https://doi.org/10.2174/1389450117666160715152503.

[58] X.N. Shi, H. Li, H. Yao, X. Liu, L. Li, K.S. Leung, H.F. Kung, D. Lu, M.H. Wong, M.C. M. Lin, In silico identification and *in vitro* and *in vivo* validation of anti-psychotic drug fluspirilene as a potential CDK2 inhibitor and a candidate anti-cancer drug, PLoS One 10 (2015), e0132072, https://doi.org/10.1371/journal.pone.0132072.

[59] G. Bethune, D Bethune, N. Fau - Ridgway, N Ridgway, Z. Fau - Xu, Z. Xu, Epidermal growth factor receptor (EGFR) in lung cancer: an overview and update, J. Thorac. Dis. 2 (2010) 48–51, 2017, https://pubmed.ncbi.nlm.nih.gov/22263017/.